Journal of Engineering Science and Technology
Vol. 8, No. 1 (2013) 77 - 92

COMBUSTION ANALYSIS OF ALGAL OIL METHYL ESTER IN A DIRECT INJECTION COMPRESSION IGNITION ENGINE

HARIRAM V.[1,*], G. MOHAN KUMAR[2]

[1]Hindustan College of Engineering, Chennai, Tamil Nadu, India
[2]Park College of Engineering & Technology, Kaniyur, Coimbatore, Tamil Nadu, India
*Corresponding Author: connect2hariram@gmail.com

Abstract

Algal oil methyl ester was derived from microalgae (Spirulina sp). The microalga was cultivated in BG 11 media composition in a photobioreactor. Upon harvesting, the biomass was filtered and dried. The algal oil was obtained by a two step solvent extraction method using hexane and ether solvent. Cyclohexane was added to biomass to expel the remaining algal oil. By this method 92% of algal oil is obtained. Transesterification process was carried out to produce AOME by adding sodium hydroxide and methanol. The AOME was blended with straight diesel in 5%, 10% and 15% blend ratio. Combustion parameters were analyzed on a Kirloskar single cylinder direct injection compression ignition engine. The cylinder pressure characteristics, the rate of pressure rise, heat release analysis, performance and emissions were studied for straight diesel and the blends of AOME's. AOME 15% blend exhibits significant variation in cylinder pressure and rate of heat release.

Keywords: Spirulina sp, Combustion, Transesterification, Photobioreactor, Biodiesel.

1. Introduction

A continuous increase in the number of vehicle along with increased global demands for fossil fuel, depletion of petroleum crudes and stringent government policies towards emission resulted in the usage of biodiesel in engine. Biodiesel encountered some major hurdles like cultivation of sources, growth phase, harvesting and extraction. Due to these problems the microalgae replaces itself as a suitable replacement for biodiesel through vegetables and crops. The biofuel from algae finds a prominent place in the future fuel due to the presence of hydrocarbon chain similar to diesel and triglycerides. There are various types of microalgae's like Chlorella sp., Spirulina sp., Scenedesmus sp., and many more [1]. The growth

Nomenclatures

C_p	Specific heat at constant pressure, J/kg K
C_v	Specific heat at constant volume, J/kg K
$\dot{m}$	Mass flow rate, kg/s
p	Cylinder pressure
Q_{ch}	Fuel chemical energy release or gross heat release
r_c	Compression ratio
t	Time, s

Abbreviations and Symbols

AO	Algal oil
AOME	Algal oil methyl ester
ASTM	American standard of testing methods
aTDC	After Top dead center
BG11	Blue Green medium
bTDC	Before Top dead center
CA	Crank angle
$CaCL_2$	Calcium chloride
CaO	Calcium oxide
CI	Compression Ignition
$CuSO_4$	Copper sulphate
EDTA	Ethylene diamine tetra acetic acid
FAME	Fatty acid methyl ester
H_3BO_3	Boric acid
K_2HPO_4	Dipotassium phosphate
MgO	Magnesium oxide
$MgSO_4$	Magnesium sulphate
$MnCL_2$	Manganese chloride
Na_2MoO_4	Sodium molybdate
RHR	Rate of heat release
$ZnSO_4$	Zinc sulphate

of microalgae is photosynthetic, i.e., it utilizes sunlight to grow and thereby also helps in global warming. The production of microalgae has been discussed worldwide in three main types; they are open pond, flat photobioreactor and tubular photobioreactor as given by Chaumont [2]. The production cost of algal oil on large scale has been reported to be comparable with biodiesel from vegetable oil which makes it promising fuel of the future. A brief study has been conducted for the production of FAME's with CaO and MgO as a catalyst. The use of straight vegetable oil in compression ignition engine results in choking, carbon deposition, vaporization and clogging of fuel injector in the combustion chamber. This can be minimized by reducing the viscosity of the oil by pyrolysis, transesterification, and thermal cracking in which transesterification is widely adopted and proven method. During transesterification reaction, the triglycerides are converted into monoesters and glycerol in the presence of sodium hydroxide as a catalyst as explained by Sahoo [3] and Graboski [4].

Extensive research has been carried out in testing the feasibility of dual fuel (biogas and biofuel) in a compression ignition which indicates the peak pressure and the heat release pattern were almost similar throughout the entire range of

loading conditions. The advantage over the use of dual fuel was lowering the NO_x to a certain extent. It has also been reported that maximum cylinder pressure, maximum rate of pressure rise and rate of heat release was higher for biodiesel at low loading condition during premixed combustion phase but at higher loading conditions all the parameters was found to be identical with that of straight diesel [5, 6]. The monoesters of Jatropa, Karanja and Polanga oil have been tested in compression ignition engine at various loads and it was found that Polanga oil is suited with maximum peak pressure during combustion process. The ignition delay was also found to be short between 5.9^{o}CA to 4.2^{o}CA [7, 8].

It is very important to understand the effect of rate of pressure rise and rate of heat release to understand the formation and control of emission and to reduce specific fuel consumption without mush affecting the performance parameters [9, 10]. The neat and blended karanja biodiesel was tested in compression ignition in which thermal efficiency increases due to excess addition of methanol at high loading condition [11, 12]. The study was conducted in a multi cylinder direct injection diesel engine. The oxides of nitrogen were also reduced to a considerable level. In the premixed combustion stage, during the ignition delay period, the air mixes with the fuel and becomes gaseous within flammability limits. Gumus [13] that at this instant, the vaporized mixture is injected into the chamber which readily burns with increased high rate of heat release during this period.

2. Materials and Methods

The algal stain was obtained from NCIM, Pune and the morphological study was carried out. BG11 medium with the constituents containing Magnesium sulphate ($MgSO_4.7H_2O$-0.2 gms), Dipotassium phosphate (K_2HPO_4-0.2gms), Calcium chloride ($CaCl_2.H_2O$-0.1 gms), Boric acid (H_3BO_3-286 mg), Manganese chloride ($MnCl_2.4H_2O$-181 mg), Zinc sulphate ($ZnSO_4.7H_2O$-22mg), Sodium molybdate ($Na_2MoO_4.2H_2O$-39mg), and Copper sulphate ($CuSO_4.5H_2O$-8mg) was prepared and mixed with 1000 ml of distilled water and boiled to 100ml. The Ethylenediamine tetra acetic acid solution was prepared by adding 745 mg of Sodium EDTA and 557 mg of ferrous sulphate in one liter of distilled water and boiled it 100ml. Both the solutions are mixed thoroughly and are maintained at pH level of 7.5. The algal stain was allowed to grow in the media. At a cell count of 10^6 cell/mL, the solution was transferred into the open pond system with proper sunlight and nutrients are supplied till the cell count reaches 10^9 cell/mL by photosynthetic process of chlorophyll A and B leaving out CO_2, .The growth phase was confirmed by placing 1 ml of algal culture in a colony counter and the optical density of the culture were also taken into account as suggested by Volkman et al. [14]. Then the algal biomass was harvested and dried. Hexane and ether solutions are added to the algal biomass and Expeller/Ultrasonication techniques are employed to separate the algal oil from biomass. The colloidal solution was kept for 48 hrs as reaction and settling time and the algal oil was filtered using an inverted separator. The AO thus obtained was heated to 80^{o}C for 2 hrs in an incubator to remove excess hexane. Transesterification reaction was initiated by adding 25% sodium hydroxide and 4% methanol to form sodium methoxide and results in the formation of AOME and washed thoroughly [15]. The transesterification reaction is enhanced by elevating the temperature upto 70^{o}C and as a result 84% of biodiesel and 16% of glycerol is obtained. The

AOME and its blends were tested for various physiochemical properties and validated against ASTM standards in Tables 1 and 2.

Table 1. Properties of AOME in Comparision with ASTM D6751 (Biodiesel) and ASTM D975 (Petro-Deisel).

S. No.	Property	Unit	AOME	ASTM D975	ASTM D6751
1	Density at 40°C	g cm^{-3}	0.8312	0.834	0.86-0.90
2	Specific Gravity at 40°C	g cm^{-3}	0.894	0.851	0.88
3	Flash point	°C	145	60-80	100-170
4	Kinematic Viscosity at 40°C	mm^2 s^{-1}	5.76	1.91-4.1	1.9-6.0
5	Water Content	%	0.04	0.02	<0.03
6	Ash Content	%	0.02	0.01	<0.02
7	Carbon Residue	%	0.03	0.17	-
8	Acid Value	mg KOH g^{-1}	0.34	0.35	0.5
9	Sulphur content	%	0.042	0.5	0.05

Table 2. Properties of Algal Oil Methyl Ester Blend with Straight Diesel.

S. No.	Fuel / Property	Cetane No.	Density g cm^{-3}	Boiling point °C	Flash point °C	Heat of combustion kJ/ kg
1	Straight Diesel	45	0.834	317	60 - 80	42000
2	AOME 5% - Diesel Blend	46.78	0.8214	268.75	62.25	41200
3	AOME 10% - Diesel Blend	47.10	0.8197	261.14	61.73	41005
4	AOME 15%-Diesel Blend	47.59	0.8168	254.32	60.49	40920

2.1. Performance in an engine

The research engine used for this study was Kirloskar single cylinder direct injection naturally aspirated compression ignition engine manufactured in Pune, India with the following configuration. The technical features of the engine are given in Table 3.

Table 3. Technical Features of Test Engine.

Model & Make	Kirloskar DM10
No of cylinder	Single cylinder direct injection
Bore (mm)	102
Stroke (mm)	118
Capacity (cc)	984
Maximum power (bhp)	10
Compression ratio (r_c)	17.5 : 1
Rated speed (rpm)	1500
Injection pressure (bar)	190-200
Injection timing	15° bTDC

The experiment was carried out with four different types of fuels, i.e., straight diesel, AOME 5% blend, AOME 10% blend and AOME 15% blend on a single cylinder, four stroke, air cooled, Kirloskar DM10 diesel engine coupled with AVL α-20 eddy current dynamometer. AVL fuel consumption meter was used to determine fuel consumption. An orifice meter coupled with a manometer was employed to measure the mass flow rate of intake air. The engine speed was measured by AVL L31 type of inductive speed pickup. AVL 654124 signal conditioning rack and piezo electric-amplifier was also employed. Kistler Make 701A type with cooling adapter and high temperature connecting cable was used for pressure measurement and inductive pulse pickup was used for crank angle and top dead center signals. AVL multipurpose amplifier and AVL 30928 crank angle calculator was employed before the data acquisition system for amplification. Twelve channel signal analyzer were used for data acquisition and the data is transferred to a personal computer for further analysis. Crypton 2000 five gas analyzer was used for measuring CO, HC and NO_x and Bosch smoke meter to measure smoke opacity. A schematic line diagram of the present study is shown in Fig. 1. The engine was operated with straight diesel and the base reading is taken. Then AOME 5%, 10% and 15% blends are tested consecutively with 20 mins of warm up time for each fuel before taking the reading.

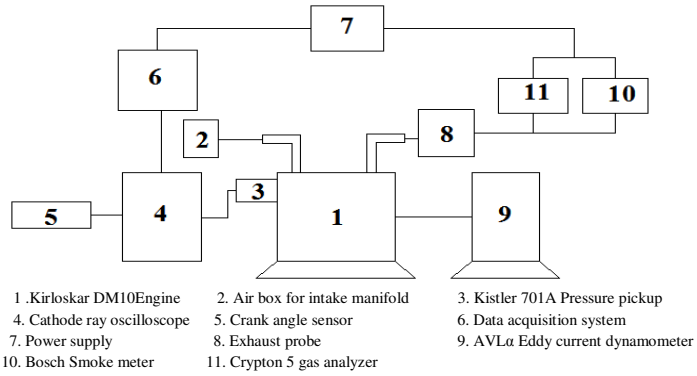

Fig. 1. Experimental Setup.

3. Results and Discussion

3.1. Effect of cylinder pressure and rate of pressure rise

Due to ignition delay, improvements were identified in the cylinder pressure and the rate of pressure rise. The ignition delay is the time duration between the openings of the valve to the sudden increase of pressure inside the combustion chamber. The pressure-crank angle figure shows the premixed combustion phase.

It can be seen that AOME 15% blend shows 2.67%, 3.81%, 4.22% and 5.31% higher peak pressure than straight diesel at 20% load, 40% load, 60% load and 80% load respectively. AOME 15% blend was performing better at all loading condition with a increase in cylinder pressure in the range of 6 to 12 bar. At high loads, the release of oxygen by AOME becomes less significant because of its change of state to atomic from molecular oxygen [16]. At full

load (80% load) the peak pressure varies between 69 bar to 73.6 bar for straight diesel and its blends with AOME as shown. AOME 15% blend shows maximum cylinder pressure at 73.6 bar at full load condition. When the blending ratio was increased more than 20% AOME to straight diesel, the combustion analysis shows 8% negative improvement which may be due to poor solubility of AOME in diesel and reduction in calorific value of AOME blends as shown in Fig. 3.

The variation in the heat of combustion readily affects the enthalpy of combustion with more quantity of oxygen addition at higher blend ratio [17]. The decrease in heat of combustion results in admittance of more fuel inside the combustion chamber to get the same power output. From Figs. (2-4) it can be also seen that the variation in pressure is between 5 to 7 bar for all AOME blends which is also due to increase in Cetane number than straight diesel, in turn influences the ignition delay and enhances premixed combustion [18]. It shows 1.5% variation with negative pressure of straight diesel. At part load, the maximum cylinder pressure was found to be 68.2 bars at 7.6°CA after TDC for AOME 15% blend against 63.2 bar at 7.7°CA after TDC for straight diesel. It is noted that the peak pressure for all blending ratio and loading condition falls between 6°CA to 7°CA which ensures safer engine operation. If the maximum pressure lies close to TDC, it may result in diesel knock. During 60% loading condition, the variation of pressure for AOME blends and straight diesel are almost similar which varies between 3.1 bars to 3.19 bar. At full load condition, the pressure variation shows almost negligible effect when compared with straight diesel and AOME blends. Under normal circumstances, 62% to 85% of fuel is at vaporized stage during the start of combustion. During combustion the percentage of vaporization increases to more than 92% in a very short duration of time [19]. From Table 2, it has be noticed that the heat of combustion decreases, but the Cetane number of the fuel steadily increases which reduces the ignition delay period and causes to raise the in-cylinder pressure and heat release rate to a certain extent.

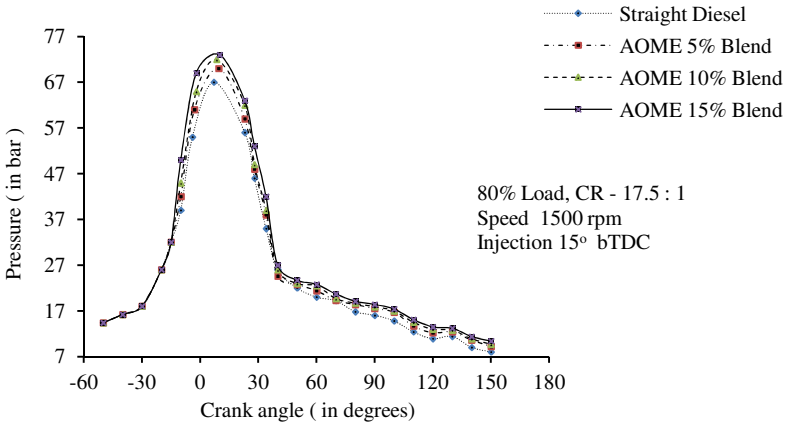

Fig. 2. Comparison of Cylinder Pressure for Straight Diesel, AOME 5%, 10% and 15% Blends at 80% Load.

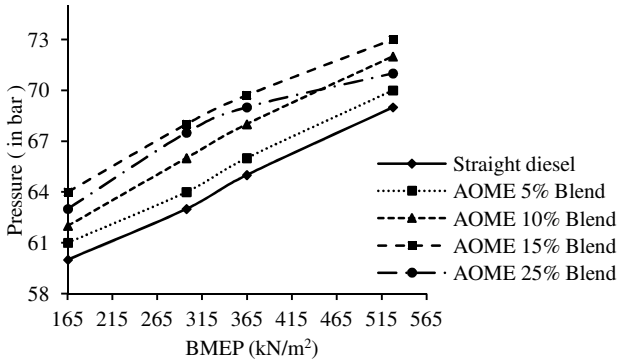

Fig. 3. Comparison of In-Cylinder Peak Pressure for Straight Diesel, AOME 5%, 10% and 15% Blends.

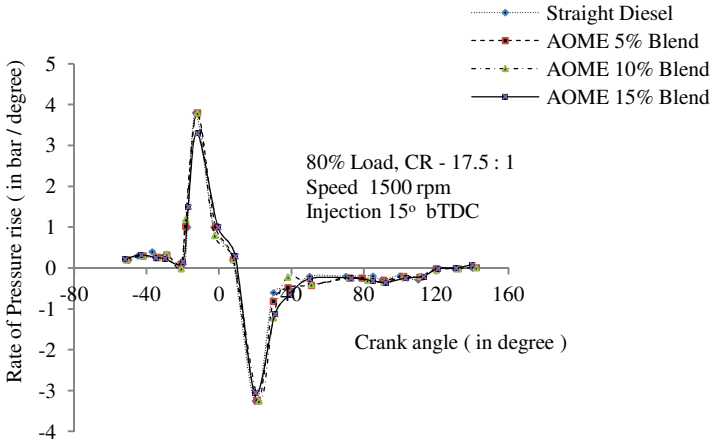

Fig. 4. Comparison of Rate of Pressure Rise for Straight Diesel, AOME 5%, 10% and 15% Blends at 80% Load.

3.2. Effect of rate of heat release

The rate of heat release is calculated using Eq. (1)

$$\frac{dQ_{ch}}{dt} = \frac{\gamma}{\gamma-1} p \frac{dV}{dt} + \frac{1}{\gamma-1} V \frac{dp}{dt} \quad (1)$$

in which $\gamma = \frac{C_p}{C_v}$ for diesel is 1.32 $\frac{dQ_n}{dt}$ = net heat release rate, kJ/deg CA , $\frac{dV}{dt}$ = rate of work transfer done by the system due to system boundary displacement, *P* is the instantaneous cylinder pressure (Pa) and *V* is instantaneous cylinder volume (m^3).The rate of heat release mainly depends on three stages. In the primary stages, the rate of heat release is very high which last only 7°CA to 8°CA. the secondary stage expels more amount of heat and remains up to 40°CA. The tertiary stage is a diminishing one which releases only 15% to 20% of the total heat. It is noted that maximum temperature of gaseous fuel for a particular brake mean effective pressure varies slightly with the increase of blend ratio of AOME.

Figures (5-8) show rate of heat release for straight diesel, AOME 5%, 10% and 15% blends at 20% load, 40%, 60% and 80% loading conditions. It is also noted that the maximum RHR for diesel is lower than blends of AOME for all loading conditions (Table 3). The RHR for straight diesel, AOME 5%, 10% and 15% at low load is found to be 35.3 kJ/deg CA, 36.20 kJ/deg CA, 37.5 kJ/deg CA and 38.6 kJ/deg CA respectively and at full load condition, the RHR for straight diesel, AOME 5%, 10% and 15% occurs at 41.95 kJ/deg CA, 43.92 kJ/deg CA, 44.12 kJ/deg CA and 46.25 kJ/deg CA respectively. The ignition delay occurs when more quantity of blended fuel is accumulated before combustion and is also resulted in the maximum RHR at higher blend ratio (AOME 15%). It is also noted that the straight diesel varies with all blends of AOME at 8% to 12% as shown because of the increase in evaporation heat of the fuel blend due to addition of AOME [20].

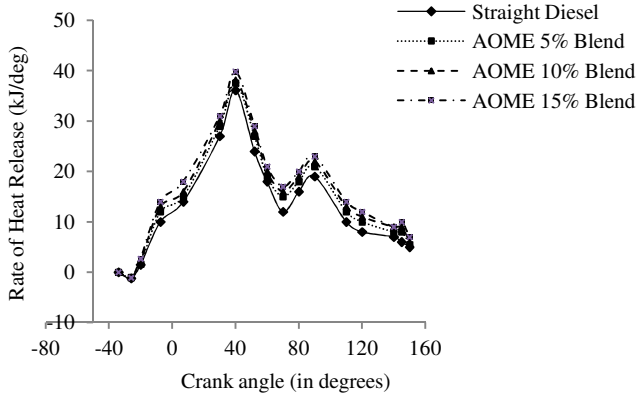

Fig. 5. Comparison of Rate of Heat Release for Straight Diesel, AOME 5%, 10% and 15% Blends at 20% Load.

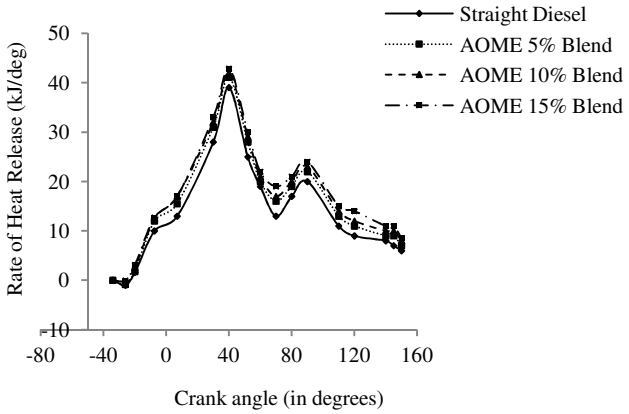

Fig. 6. Comparison of Rate of Heat Release for Straight Diesel, AOME 5%, 10% and 15% Blends at 40% Load.

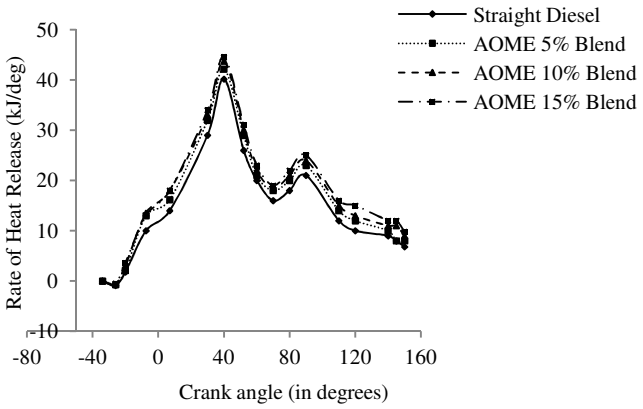

Fig. 7. Comparison of Rate of Heat Release for Straight Diesel, AOME 5%, 10% and 15% Blends at 60% Load.

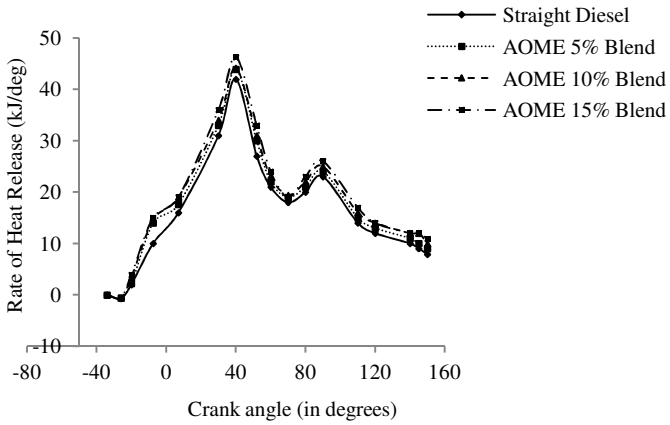

Fig. 8. Comparison of Rate of Heat Release for Straight Diesel, AOME 5%, 10% and 15% Blends at 80% Load.

3.3. Comparison of brake thermal efficiency and brake Specific energy consumption

Moderate variation is noticed in thermal efficiency form 1.5% to 4%. The various blend ratios were found to have minimal effect on Power and Brake thermal efficiency (Fig. 9). The chemical bonding between carbon and oxygen plays a vital role in the supply of oxygen during the combustion, especially in the premixed combustion stage. The pressure value gives a clear picture about the rate of heat release. The combustion chamber contains oxygen in the micro air fuel particle which also enhances the combustion characteristics. The specific energy consumption of AOME 5% blend at 3KW brake power was found to be 0.285 kg/kWhr which is better than the Straight diesel (Fig. 10). As the blending ratio increases, the specific fuel consumption increases slightly higher than Straight diesel which indicates the presence of more atomic oxygen in the fuel particles. The

brake thermal efficiency also shows minor variation with the base diesel and the blends of AOME. The BTE of base diesel was found to be 28% at 3KW brake power. AOME 15% blend shows a better efficiency throughout the entire study. At AOME 5% and 10% blends, there is moderate variation in brake thermal efficiency which may be due to release of oxygen too early [21].

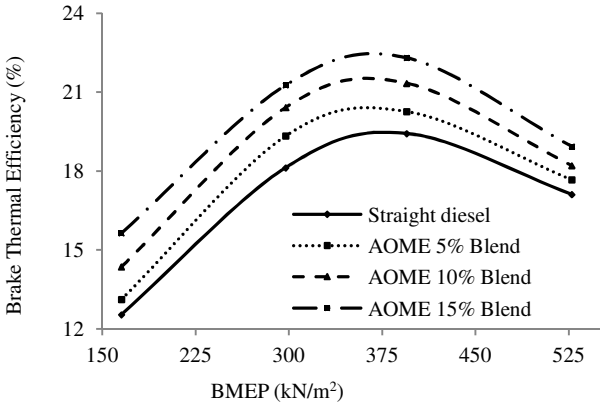

Fig. 9. Comparison of Brake Thermal Efficiency and BMEP.

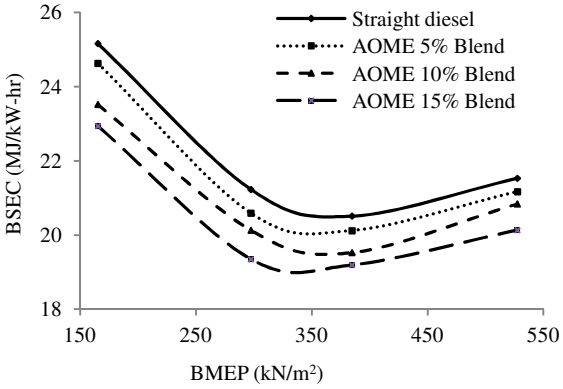

Fig. 10. Comparison of BSEC and BMEP.

3.4. Comparison of HC, CO, NOx, smoke and particulate emission

3.4.1. HC emission

The AOME 15% blend was found to be more effective in reducing the HC emission at 16% (Fig. 11). The hydrocarbon emission for straight diesel is 55 ppm at 4.2 kW BP while AOME 15% blend shows only 48 ppm. At higher blend ratio, AOME supply more quantity of oxygen which will result in less HC emission. The HC emission of base diesel is higher because of the absence of

oxygen content. At mid range BP, the emission of HC is almost similar for 5%, 10% and 15% AOME blends.

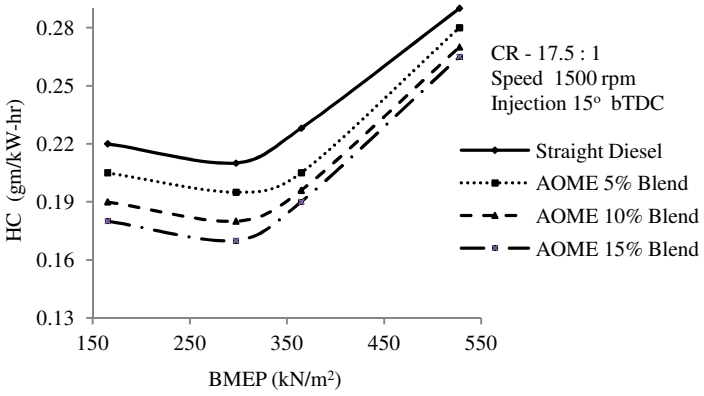

Fig. 11. Variation of HC Emission.

3.4.2. CO emission

All the blending ratio of AOME has significant effect on CO emission. At higher blending levels AOME 15% diesel blends seems to have less CO emission than the other two blends (Fig. 12). At maximum brake power, 0.025% of CO is emitted by AOME 10% blend while the straight diesel emits more than 0.1% CO and the leaner blends of AOME emits 0.05% to 0.06% of CO which may be due to less time interval for CO to become CO2.

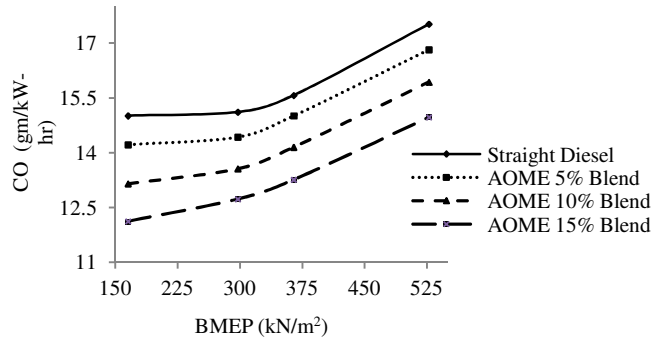

Fig. 12. Variation of CO Emission.

3.4.3. NO_x emission

The effect of AOME on oxides of nitrogen is very minimal. AOME 15% blend shows 8% more emission of NOx (Fig. 13). This may be due to decrease in density of blended fuel which results in fine atomization and combustion advancement. The peak temperature was found to be high at higher blend ratios. The increase in Cetane number decreases the ignition delay and maximum

pressure inside the cylinder increases producing more quantity of NOx. It is also noted that AOME 15% blend emits 120 ppm more quantity of NOx than straight diesel. The lower blends of AOME have similar effect in the formation of NO_x.

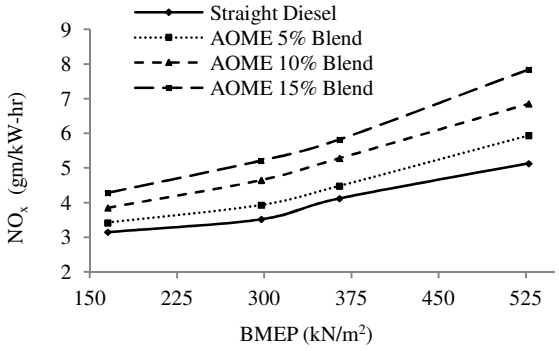

Fig. 13. Variation of NO_x Emission.

3.4.4. Smoke emission

By increasing the AOME blends, the diffusive combustion phase is shortened thereby resulting in reduction of smoke at higher blend ratios. Also at higher blend ratio, oxidation of smoke takes place due to liberation of more quantity of oxygen.

The premixed combustion, Cetane number and ignition delay plays a vital role at increased AOME blends and thereby helps in reduction of smoke and enhances combustion. The smoke emissions are higher for straight diesel and as the blend ratio of AOME increases, the smoke readings are reduced with increase in load (Fig. 14). The increase of smoke at higher loads may be due to change of state of oxygen from diatomic to mono-atomic state which will not take part in combustion and oxidation of smoke will reduce at high loads. AOME 15% blend level shows lesser emission of smoke at part load when compared with other loading conditions. AOME 20% blend shows higher emission of smoke at all load because of reduction in peak pressure and heat release rate.

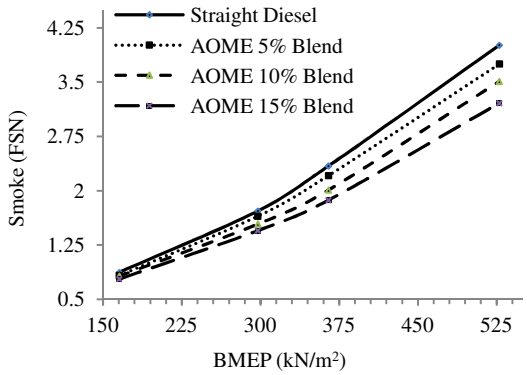

Fig. 14. Variation of Smoke Emission.

3.4.5. Particulate emission

At higher AOME blend ratio, soot oxidation takes place because of the presence and liberation of more oxygen atoms to the local fuel particles during combustion especially in low and part load condition (Fig. 15). At high loading condition, the oxygen disintegration into mono-atomic oxygen which will not help in oxidation reaction and leads to more soot formation. AOME 15% blend ratio at low and part load was found to reduce soot formation to a great extent. When the AOME blend ratio is increased beyond 15%, the soot formation was drastically increased because of poor solubility of oxygen with the fuel particles [17]. The oxygen molecules could not able to break the chemical bond to oxidize the soot formation at all load conditions. Cetane number and ignition delay also affects the soot formation to a great extent because the time for evaporation of fuel is affected.

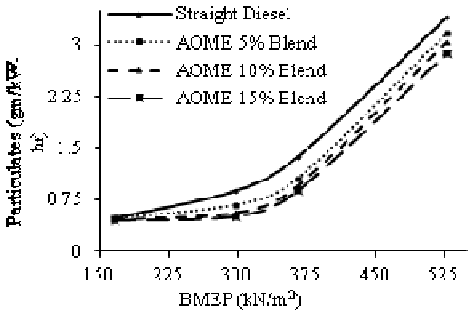

Fig. 15. Variation of Particulates Emission.

3.5. Estimation of Uncertainty

The uncertainty is measured based on Gaussian distribution method, Eq. (2) with a confidence limit of $\pm 2\sigma$, i.e., 96% of measured data lie within limits of 2σ of mean value [22]. The uncertainty for instruments used and measuring parameters are given in Tables 4 and 5 and the overall uncertainty for the experiment is calculated as ±1.4.

$$\Delta R = \sqrt{\left[\left(\frac{\partial R}{\partial X_1}\Delta X_1\right)^2 + \left(\frac{\partial R}{\partial X_2}\Delta X_2\right)^2 + \cdots \left(\frac{\partial R}{\partial X_n}\Delta X_n\right)^2\right]} \quad (2)$$

Table 4. Details of Uncertainty of Measured Parameters.

S. No.	Measurements	% of Uncertainty
1	Speed	±0.12
2	Load	±0.47
3	Mass flow rate of air	±0.62
4	Mass flow rate of fuel	±0.89
5	Brake power	±0.25
6	Brake thermal efficiency	±0.25
7	NO_X	±1.10
8	HC	±0.014
9	CO	±0.83
10	Smoke	±2.1

Table 5. Uncertainty and Accuracy Range of Instruments.

S. No.	Instruments	Range	Accuracy	% of Uncertainty
1	Speed measurement	0-10000	+10 to -10 rpm	±0.1
2	Exhaust gas	0-900 ^{o}C	+1 ^{o}C to -1 ^{o}C	±0.16
3	Smoke measurement	BSU 0-10	+0.1 to -0.1	±1.0
4	Stop watch	-	+0.5s to -0.5s	±0.2
5	Pressure transducer	0-110 bar	+0.1 kg to -0.1	±0.1

4. Conclusions

In the present work, biodiesel from microalgae is determined to be suitable replacement to petro-diesel and vegetable oils. The BG11 medium was found to yield good biomass of algae. The extracted AOME was found to meet the standards of ASTM. The cylinder pressure was found to be maximum at higher blending ratio of AOME.

- The rate of pressure rise is identified to be varying between 6.5% to 8% at all loading condition and for all blending ratio.
- During part load condition, the variations of peak pressure were almost similar to all blends.
- The RHR is maximum at higher blend ratio (AOME 15%) because increase in evaporation heat of the fuel blends.
- The oxygen content in AOME helps in the premixed combustion phase to progress in a better way which leads to better combustion. The increase in cylinder is about 10 to15 bar, the maximum rate of pressure rise is between 2% to 4% and the rate of heat release is between 5% to 8% for higher blend ratios.
- The increase in Cetane number of the fuel increases the ignition delay and thereby the peak pressure inside the cylinder also increases.
- The BTE and BSEC for AOME 15% shows positive improvement on comparison with straight diesel.
- The emissions of HC, CO, Smoke and Particulate decreases with a slight increase in NO_x.

References

1. Norsker, N.-H.; Barbosa, M.J.; Vermue, M.H.; and Wijffels, R.H. (2011). Microalgal production - A close look at the economics. *Biotechnology Advances*, 29(1), 24-27.
2. Chaumont, D. (1993). Biotechnology of algal biomass production: a review of systems for outdoor mass culture. *Journal of Applied Phycology*, 5(6), 593-604.
3. Sahoo, P.K.; and Das, L.M (2009). Combustion analysis of jatropha, karanja, and polanga based biodiesel as fuel in a diesel engine. *Fuel*, 88(6), 994-999.

4. Graboski, M.S.; and McCormick, R.L. (1998). Combustion of fat and vegetable oil derived fuels in diesel engines. *Progress in Energy and Combustion Science*, 24(2), 125-164.
5. Canakci, M. (2007). Combustion characteristics of a turbocharged DI compression ignition engine fueled with petroleum diesel fuels and biodiesel. *Bioresource Technology*, 98(6), 1167-1175.
6. Radu, R.; Petru, C.; Edward, R.; and Gheorghe, M. (2009). Fueling an DI agricultural diesel engine with waste oil biodiesel: effects over injection, combustion and engine characteristics. *Energy Conversion Management*, 50(9), 2158-2166.
7. Nwafor, O.M.I. (2003). The effect of elevated fuel inlet temperature on performance of Diesel engine running on neat vegetable oil at constant speed conditions. *Renewable Energy*, 28(2), 171-181.
8. Agarwal, A.K.; and Das, L.M. (2001). Biodiesel development and characterization for use as a fuel in compression ignition engine. Transaction of the ASME. *Journal of Engineering for Gas Turbine and Power*, 123(2), 440-447.
9. Hariram, V.; and Kumar, G.M. (2010). The effect of algal oil diesel blends on combustion process and emission characteristics in single cylinder naturally aspirated diesel engine. *iCIRET* 2010, 1-6.
10. Kumar, G.M.; and Hariram, V. (2011). Experimental investigation of algal oil diesel blends on combustion process and emission parameters in a single cylinder diesel engine. *CiiT International Journal of Automation and Autonomous System*, 3(1), 43-47.
11. Graboski, M.S.; and McCormick, R.L. (1998). Combustion of fat and vegetable oil derived fuels in diesel engines. *Progress in Energy and Combustion Science*, 24(2), 125-164.
12. Balat, H. (2010). Prospects of biofuels for a sustainable energy future: a critical assessment. *Energy Education Science and Technology Part A*, 24(2), 85-111.
13. Gumus, M. (2010). A comprehensive experimental investigation of combustion of heat release characteristics of a biodiesel (hazelnut kernel oil methyl ester) fueled direct injection compression ignition engine. *Fuel*, 89(10), 2802-2814.
14. Volkman, J.K.; Jeffrey, S.W.; Nichols, P.D., Rogers, G.I.; and Garland, C.D. (1989). Fatty acid and lipid composition of 10 species of microalgae used in mariculture. *Journal of Experimental Marine Biology and Ecology*, 128(3), 219-240.
15. Puhan, S.; Vedaraman, N.; Ram, B.V.B.; Sankarnarayanan, G.; and Jeychandran, K. (2005). Mahua oil (Madhuca Indica seed oil) methyl ester as biodiesel-preparation and emission characteristics. *Biomass and Bioenergy*, 28(1), 87-93.
16. Yu, C.W.; Bari, S.; and Ameen, A. (2002). A comparison of combustion characteristics of waste cooking oil with Diesel as fuel in a direct injection Diesel engine. *Proceedings of the Institution of Mechanical Engineers D: Journal of Automobile Engineering*, 216(4), 237-243.

17. Barsic, N.J.; and Lumke, A.L. (1981). Performance and emissions characteristics of a naturally aspirated diesel engine with vegetable oil fuels. *SAE Technical paper No*. 810262.
18. Senatore, A.; Cardone, M.; Rocco, V.; and Prati, M.V. (2000). A comparative analysis of combustion process in DI diesel engine fueled with biodiesel and diesel fuel. *SAE Technical paper No*. 2000-01-0691.
19. Heywood, J.B. (1988). *Internal combustion engine fundamentals*. (1st Ed.). McGraw Hill.
20. Qi, D.H.; Geng, L.M.; Chen, H.; Bian, Y.ZH.; Liu, J.; and Ren, X.CH. (2009). Combustion and performance evaluation of diesel engine fuel with biodiesel produced from soyabean crude oil. *Renewable Energy*, 34(12), 2706-2713.
21. Benjumea, P.; Agudelo, J.; and Agudelo, A. (2009). Effect of altitude and palm oil biodiesel fuelling on the performance and combustion characteristics of a HSDI diesel engine. *Fuel* 88(4), 725-731.
22. Monyem A.; and Van Gerpen, J.H. (2001). The effect of biodiesel oxidation on engine performance and emissions. *Biomass and Bioenergy*, 20(4), 317-325.